Ultra-Compact Variable All-optical Attenuator Based on Multimode Interference Couplers on an SOI Platform

Trung-Thanh Le

***Abstract*—In this paper, two methods for obtaining an ultra-compact variable all-optical attenuator based on multimode interference (MMI) using silicon waveguides are proposed. The first method is to use two connected silicon waveguides. The second method is to use a multimode interference coupler. B forming a surface pattern on the top of the MMI region at special positions or on the top of linking waveguides, a variable attenuator is achieved. The device dimension is about 2 μm x30 μm that is the smallest length of an optical attenuator reported up-to-date. Designs of the proposed devices on silicon on insulator (SOI) platform are then verified and optimized using numerical simulation methods.**

***Index Terms*—Optical computing, multimode interference (MMI) couplers, optical attenuator, SOI waveguide, CMOS technology, Beam propagation method (BPM).**

I. Introduction

The variable optical attenuator (VOA) is widely used to adjust the existing power and wavelength in-long haul optical communication systems. Previous papers have reported several typical VOAs based on microelectro-mechanical systems [1], liquid crystals [2], waveguides, thermo-optic effect [3], plasmonic waveguides [4] and multimode interference coupler [5]. However, these variable optical attenuators have large size and the difficulty of integration in photonic integrated circuits.

In recent years, MMI structures have been widely used in a number of optical communication applications due to their advantages of compactness, relaxed fabrication tolerances and easy integration. These applications include optical couplers, wavelength monitors for wavelength division multiplexing systems, Mach-Zehnder interferometer (MZI) modulators and switches and optical gates [6],[7].

In addition, in this paper, silicon on insulator (SOI) technology is used for the design of MMI devices. Silicon photonics [8, 9] was chosen because the fabrication of such devices require only small and low cost modifications to existing fabrication processes. SOI technology is compatible with existing complementary metal–oxide–semiconductor (CMOS) technologies for making compact, highly integrated, and multifunction devices [10], [11]. The SOI platform uses silicon both as the substrate and the guiding core material. The large index contrast between Si (n_{Si} =3.45 at wavelength 1550nm) and SiO_2 (n_{SiO_2} =1.46) allows light to be confined within submicron dimensions and single mode waveguides can have core cross-sections with dimensions of only few hundred nanometers and bend radii of a few micrometers with minimal losses. Moreover, SOI technology offers potential for monolithic integration of electronic and photonic devices on a single substrate.\

Manuscript received December 25, 2011; revised April 16, 2012.

Trung-Thanh Le is with the Faculty of Information Technology, Hanoi University of Natural Resources and Environment, 41A K1 Phu Dien Road, Tu Liem, Ha Noi, Viet Nam (Email: thanh.le@hunre.edu.vn)

II. Theory

Optical attenuators can be created by introducing a section of loss waveguide into the input waveguide. This may be achieved by suitable doping of the silicon channel waveguide. Another method of achieving attenuation is to use a wide multimode waveguide of non-resonant length (i.e. an unfocussed MMI). Loss then may occur at the junction of the multimode section and the single mode waveguide. In the following example, a width W_2 from 600nm to 1000nm is chosen to keep the device fairly compact. The amount of power lost scales with the length of the wider waveguide section W_2. It is assumed that the waveguide cross-section used in the design is shown in Fig.1, where the core thickness is $h_{co} = 220\text{nm}$ and operating wavelength is $\lambda = 1550\text{nm}$.

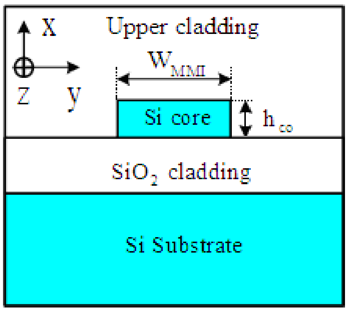

Fig. 1. Silicon waveguide cross-section used in the designs

Fig. 2(a) shows the design of such a device and Fig. 2(b) shows the normalized output power of the device as a function of distance along the propagation direction for different waveguide widths W_2 calculated by the three-dimensional beam propagation method (3D-BPM). For example, the 3D-BPM simulation result for waveguide widths $W_1 = 450\text{nm}$ and $W_2 = 1\mu\text{m}$ at a waveguide length of 5μm is shown in the insert box in Fig. 2(b). It is clear that by adjusting the width, an attenuator is created. Note that there is a peak at a width of 900nm for a length of 5μm in the results. The reason is that this length is near the length to achieve a single image at the output (a resonant length). As a result, the signal amplitude can be changed by simply choosing an appropriate length for the wider waveguide section. If it is important to maintain a certain relative phase, then it is necessary to determine the phase shift introduced by this amplitude attenuator. It can also be calculated by using the 3D-BPM method.

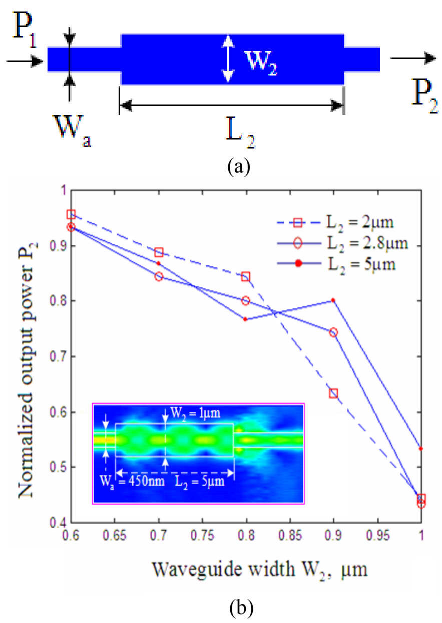

Fig. 2. Optical attenuator using a wide waveguide (a) structure of an optical attenuator on the silicon channel waveguide and (b) normalized output power P_2 at different waveguide widths W_2 and lengths L_2 of the wide waveguide

It is clear from Fig. 2(b) that power is lost to radiation modes. Therefore, in practice it may be necessary to take steps to absorb or reflect this radiated power so that it does not interfere with other components on the same chip.

In this study, an optical attenuator can be realized by using an 1x1 MMI coupler formed by cascading 1x2 and 2x1 MMI structures. Fig. 3 shows a diagram of such an optical attenuator. In principle, adding a phase shifter to the linking waveguides enables the power at the output port to be controlled by changing the phase $\Delta\varphi$ of the phase shifter. It is easy to show that, based on the transfer matrix method, the complex amplitude b_1 of the signal at the output port is calculated by

$$b_1 = [\cos(\frac{\Delta\varphi}{2}) e^{j(\frac{\Delta\varphi}{2}+\phi_0)}] a_1 \quad (1)$$

where a_1 is the complex amplitude of the signal at the input port and ϕ_0 is the constant phase factor introduced by the MMI coupler.

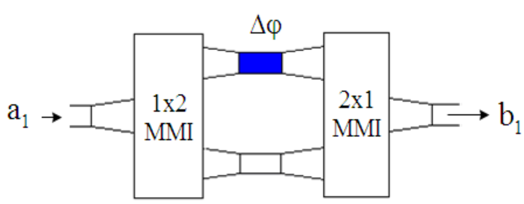

Fig. 3. Optical attenuator based on the MZI structure

It is highly desirable to reduce the size of the circuit as much as possible. In the present work, a modified structure is proposed for implementing an optical attenuator using the 1x1 MMI structure as shown in Fig. 4. The surface pattern technique will be employed to vary the output amplitude [12]. The field of the two images at the length of $L_{MMI}/2$ can be expressed by

$$\psi(x,z) = \frac{1}{\sqrt{2}} \psi_0(x + W_{MMI}/4, 0) e^{j\phi_1} + \frac{1}{\sqrt{2}} \psi_0(x - W_{MMI}/4, 0) e^{j\phi_2} \quad (2)$$

where $a_1 = \psi_0(x,0)$ is the input field and W_{MMI} is the width of the MMI coupler.

In the following design, the width of the MMI structures is chosen to be $W_{MMI} = 2\mu m$. As a result, the optimised length for obtaining a 1x1 MMI coupler is $L_{MMI} = 7.6\ \mu m$. The optimised length for obtaining a 1x2 MMI coupler is $3.8\ \mu m$.

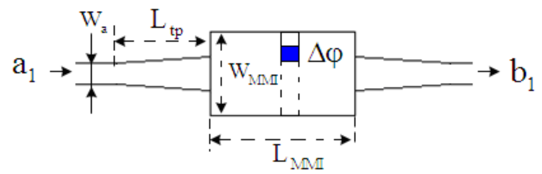

Fig. 4. Modified structure of an optical attenuator, where a pattern region introduces a phase shift $\Delta\varphi$ (darker colour)

In this paper, the surface pattern technique is employed to make a phase shift of $\Delta\varphi$ [12]. By forming a surface pattern on the top of the MMI region at special positions or on the top of linking waveguides (SOI channel waveguides), any desired phase shift can be produced [12]. The refractive index is adjusted by changing the etch depth; etch width and/or the length of these patterns. The advantages of this approach are that the etching can be done after the device has been fabricated and patterns introduce only low additional loss. In addition, by using suitable masks, only one additional simple process step is required.

By using the 3D-BPM simulation, the effective refractive indices for the transverse electric (TE) fundamental mode for different waveguide thicknesses, but the same width of 480nm, are plotted in Fig. 5(a). The simulations show that the effective refractive index is directly proportional to the waveguide thickness. This is the operating principle of introducing a phase shift using the surface pattern technique. If a pattern region has a thickness of $h_{pt} = 180nm$, the effective refractive index of the fundamental mode within this waveguide section will be changed (compared to the standard waveguide with a thickness of $h_{co} = 220nm$). The mode profiles of the fundamental TE mode of the waveguide at $h_{co} = 220nm$ is plotted in Fig. 5(b).

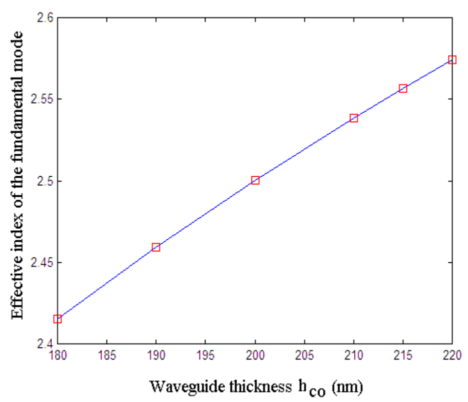

(a)

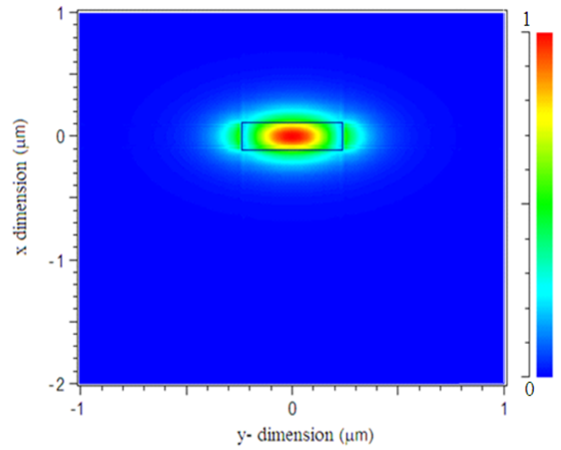

(b)

Fig. 5. (a) The effective indices of the fundamental TE mode at different waveguide thicknesses for an SOI channel waveguide of width 480nm and (b) Field profile of the waveguide with $h_{co} = 220nm$

In order to achieve a phase shift of $\Delta\varphi = -\pi$, the length L_p of the pattern region as a function of the pattern depths h_p ($h_p = h_{co} - h_{pt}$) calculated from $L_p = \frac{\lambda}{2\pi}\frac{\Delta\varphi}{\Delta n_e}$ is shown in Fig. 6. Here, Δn_e is the difference in effective indices between that for the waveguide having a thickness h_{co} and that for the standard waveguide having a thickness of $h_{co} = 220nm$.

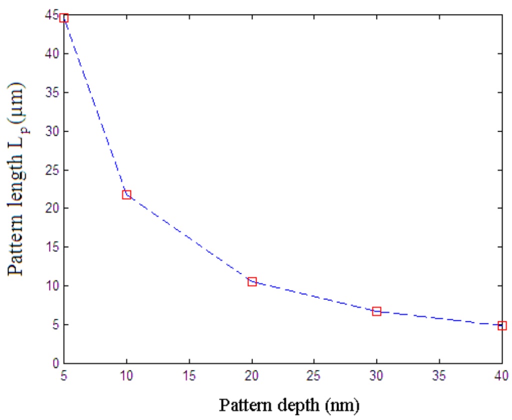

Fig. 6. Pattern length L_p required to achieve a phase shift of $-\pi$ at different depths

The 3D-BPM simulation result (Fig. 7) shows that at a pattern length of $L_p = 10\mu m$, the loss of the signal propagating through the pattern section is only 0.043dB. A pattern depth of $h_p = 40nm$ is used throughout this chapter. These dimensions are suitable for practical fabrication.

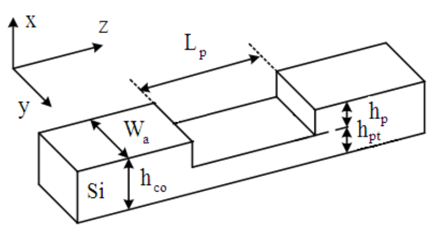

(a)

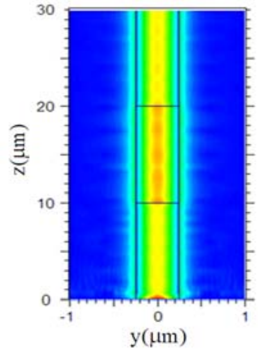

(b)

Fig. 7. Pattern used for introducing a phase shift (a) structure of the pattern region and (b) power distribution through a pattern having a length of $L_p = 10\mu m$

In order to locate the most suitable region for the surface pattern, the 3D-BPM is used. Fig. 8(a) plots the field propagation through an 1x1 MMI structure having a width of $2\mu m$ and a length of $7.6\mu m$. The excess loss is 0.03dB for this case. The central position of the pattern therefore is at the MMI length of $3.8\ \mu m$. It is assumed that the device is designed on an SOI channel waveguide structure. The access waveguide has a width of 450nm and a thickness of 220nm. Tapered waveguides are used to improve the device performance. A taper length of 5μm is chosen. In this design, a pattern having a width of 450nm and a depth of 40nm is used. The normalized optical power at the output port at different pattern lengths can be calculated as shown in Fig. 8(b).

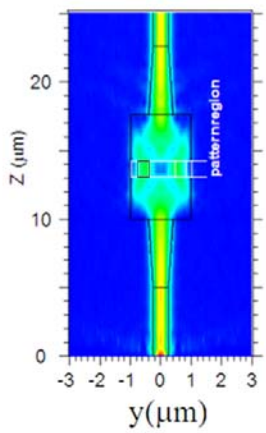

(a)

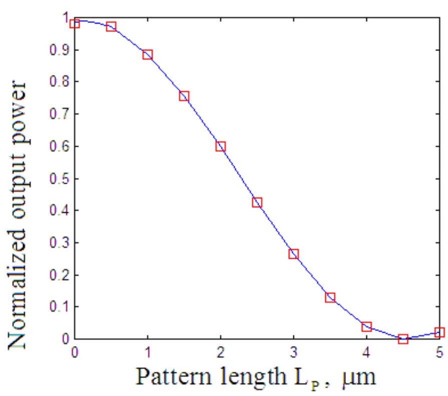

(b)

Fig. 8. Power distribution in a multimode waveguide having a width of $2\mu m$ (a) determination of locations of the pattern region and (b) normalized output power at different pattern lengths

The power distributions inside such a device, having pattern lengths of $0.5\mu m$ and $1.5\mu m$, are shown in Fig. 9(a) and 9(b), respectively. The normalized output power is 0.98 for the pattern length of $0.5\mu m$ and 0.73 for the pattern length of $1.5\mu m$.

Note that if the output is to be compared with other signals in an optical logic system, then the phase associated with the optical attenuators may need to be compensated for at the output.

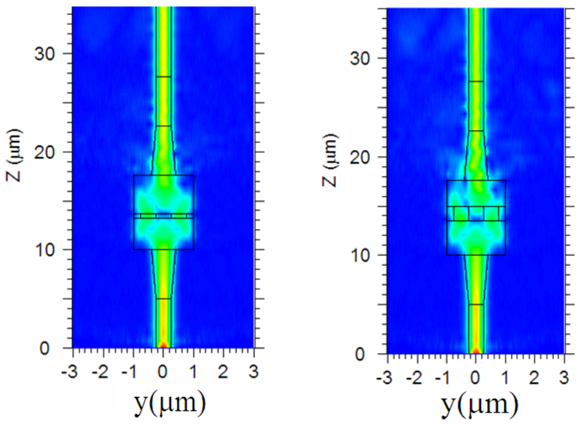

Fig. 9. Power distribution inside optical attenuators for two cases (a) a pattern length of $0.5\mu m$ and (b) pattern length of $1.5\mu m$

III. Conclusion

In this paper, we have proposed two methods for realizing ultra-compact variable all-optical attenuators based on MMI structures using CMOS technology. The designs for these devices have been implemented on the silicon on insulator platform and the 3D-BPM was used to optimise the device structures. The proposed devices can be useful building blocks for all-optical signal processing applications such as all-optical logic gates and all-optical signal transforms.

References

[1] R. Saini, A. Geisberger, and K. Tsui, "Assembled MEMS VOA," presented at IEEE/LEOS International Conference on Optical MEMS, 18-21 Aug. 2003.

[2] E. Nicolescu, M. Chongchang, A. Fardad, and M. Escuti, "Polarization-Insensitive Variable Optical Attenuator and Wavelength Blocker Using Liquid Crystal Polarization Gratings," *IEEE Journal of Lightwave Technology*, pp. 3121 - 3127, Nov.1, 2010.

[3] L. Yang, H. Xin, and Q. Fang, "New type of multimode-interference-type thermo-optic variable optical attenuator," *Optical Engineering*, vol. 43, pp. 2497-2498, 2004.

[4] K. Leosson, T. Rosenzveig, P. G. Hermannsson, and A. Boltasseva, "Compact plasmonic variable optical attenuator," *Optics Express*, vol. 16, pp. 15546-15552, 2008.

[5] X. Jiang, X. Li, and H. Zhou, "Compact variable optical attenuator based on multimode interference coupler," *IEEE Photonics Technology Letters*, vol. 17, pp. 2361 - 2363, Nov. 2005.

[6] L. W. Cahill and T. T. Le, "MMI Devices for Photonic Signal Processing," presented at 9th International Conference on Transparent Optical Networks (ICTON 2007), Rome, Italy, 1-5 July 2007

[7] T. T. Le, "The design of all-otpical NOT and OR gates based on 2x1 MMI couplers on an SOI platform," *Journal of Science and Technology, ISSN:0866 708X*, vol. 48, pp. 47-56, 2010.

[8] G. T. Reed and A. P. Knights, *Silicon Photonics: An Introduction*: John Wiley and Sons, March 2004.

[9] T. Tsuchizawa, K. Yamada, and H. F. e. al., "Microphotonics Devices Based on Silicon Micro-Fabrication Technology," *IEEE Journal of Selected Topics in Quantum Electrononics*, vol. 11, pp. 232-, 2005.

[10] S. Janz, P. Cheben, and D. D. e. al., "Microphotonic elements for integration on the silicon-on-insulator waveguide platform," *IEEE Journal of Selected Topics in Quantum Electrononics*, vol. 12, pp. 1402-1415, Dec. 2006.

[11] R. Soref, "The past, present, and future of silicon photonics," *IEEE Journal of Selected Topics in Quantum Electrononics*, vol. 12, pp. 1678-1687, Dec. 2006.

[12] T. T. Le and L. W. Cahill, "The Design of Multimode Interference Couplers with Arbitrary Power Splitting Ratios on an SOI Platform," presented at LEOS 2008, Newport Beach, California, USA, 9-14 Nov 2008.

Trung-Thanh Le received the B.Sc. and M.Sc. degrees in electronic and telecommunication engineering from Hanoi University of Science and Technology, Vietnam in 2003 and 2005, respectively. He received the PhD degree in electronic engineering from La Trobe University, Australia in 2009. He was a lecturer at the University of Transports and Communications, Hanoi, Vietnam from 2003-2010 and since 2010; he is with Hanoi University of Natural Resources and Environment and is Dean of the Faculty of Information Technology, Hanoi University of Natural Resources and Environment, Hanoi, Vietnam.